

RECENT SEISMICITY AND SLAB GAP BENEATH TOBA CALDERA (SUMATRA) REVEALED USING HYPOCENTER RELOCATION METHODOLOGY

Andrian Simanjuntak^{1,2,3}, *Umar Muksin^{2,4}, Yusran Asnawi⁵, Syamsul Rizal¹, Shengji Wei^{6,7}

¹Graduate School of Mathematics and Applied Sciences, Universitas Syiah Kuala, Indonesia

²Tsunami Disaster and Mitigation Research Center, Universitas Syiah Kuala, Indonesia

³Badan Meteorologi Klimatologi dan Geofisika, Aceh, Indonesia

⁴Department of Physics, Faculty of Mathematics and Natural Sciences, Universitas Syiah Kuala, Indonesia

⁵Department of Information and Technology Education, Ar-Raniry Islamic University, Indonesia

⁶Asian School of the Environment, Nanyang Technological University, Singapore

⁷Earth Observatory of Singapore, Nanyang Technological of Singapore, Singapore

*Corresponding Author, Received: 14 Sep. 2022, Revised: 23 Oct. 2022, Accepted: 30 Oct. 2022

ABSTRACT: The Toba Lake is located in the northern part of Sumatra with a large complex caldera that formed by a supervolcano eruption 74,000 years ago and has been influenced by a tectonic process over several centuries. The tectonic process has produced recent seismicity in various systems, one of which is the Investigator Fracture Zone (IFZ). The IFZ incorporated with Sumatra subduction as a slab tear in the vertical direction beneath Toba. Therefore, we applied the hypocenter relocation method with a 1-D seismic velocity model to figure out the detailed structure beneath Toba and along the IFZ. The results show a significant change in hypocenter quality which is around 90% of total hypocenters with RMS < 1.0s, while 60% of total hypocenters have RMS < 0.5s following an oblique angle of ~65° beneath Toba. The results strongly highlight a slab gap of Sumatra subduction that may construct a slab tear with a gap at a depth > 100 km, and indicate a shallower dip to the northwest of Toba. A possible slab tear with a slab gap can be found along IFZ as the consequence of a rheologically weak structure which varies from the north to the south.

Keywords: Subduction, Slab gap, Toba caldera, Sumatra, Hypocenter relocation, Investigator fracture zone

1. INTRODUCTION

The Toba Lake caldera is located in the northern part of Sumatra (Indonesia) and is bounded by an area of 100 km x 30 km. The caldera was formed by a supervolcano eruption with the metric volume of silicic pyroclastic around 2,800 km³ 74,000 years ago in the Quaternary period [1, 2]. The eruption resulted in a depression landmark with a surface elevation of ~900 m and a depth up to ~500 m [3]. Previously, the Toba eruption has been a debatable topic; for example, a single eruption with large impact formed the Toba caldera while there is a possible impact from multiple eruptions [3, 4]. Tectonically, the seismic activities in Sumatra Island are mostly controlled by the Indo-Australian subduction system in the NW-SE direction with a slip rate of 5 – 6 mm/yr (see Fig. 1) [5].

The position of Toba, along the Sunda arc and above a subducting slab, is consistent with the prediction that magma still occupies the crust below the caldera complex [2]. In addition, the eruption landmark of the Toba depression parallels the Sumatra Fault, which moves right-

laterally at a rate of 10-20 mm/yr [6]. The approximation slip rate near Toba is around ~2.3 cm/year with a dextral mechanism [7, 8]. Another conspicuous system known as the Investigator Ridge Fracture Zone (IFZ) is not clearly visible via bathymetry contours, but it subducts directly beneath Toba in the SW – NE direction.

A previous hypocenter distribution study clearly displays the geometry of the IFZ that incorporated with slab subduction and indicated a bend portion with high seismicity [9, 10, 11]. Geodetically, the IFZ is subducted at an oblique angle of ~65° and a velocity of 57 mm/yr below the Sumatran mainland, and the direction of the fracture zone trend near the trench is almost parallel to the convergence vector [2]. Koulakov et al. [3] assessed the IFZ as the transform zone with length 2,500 km in the Indian Ocean and its continuation to the onshore Sumatran area. Seismically, the IFZ has generated a distribution of hypocenters along the fracture line directed towards Toba with a dipping linear structure.

Several research efforts have been undertaken in Toba; for example, Fauzi et al. [9] highlight the Benioff zone beneath Toba at ~125 km depth with a 30° subducted angle; Masturyono et al. [2]

studied the caldera structure by using tomography body wave and gravity inversion; Sakaguchi et al. [10] used ambient noise to determine the crustal thickness beneath Toba that ranges from 29 to 40 km; Jaxybulatov et al. [11] highlighted the anisotropy to find the crustal structure beneath Toba; and Lange et al. [12] combined several temporary stations to highlight the subduction beneath Mentawai and the IFZ system using tomography body-wave. In this study, the current seismicity beneath and surrounding Toba was analyzed to assess the possible gap in the slab

subduction and the IFZ system that to our knowledge has not been studied previously. Many research efforts on the possibility of a slab gap have been undertaken globally; for example, a slab gap in the upper mantle beneath the Central Anatolia subduction zone, the slab gap beneath the Pampean flat subduction zone, and the slab gap under the Adria plate [13]. In order to map the deep structure beneath Toba, local and regional stations that record the seismic activities were used simultaneously in inversion.

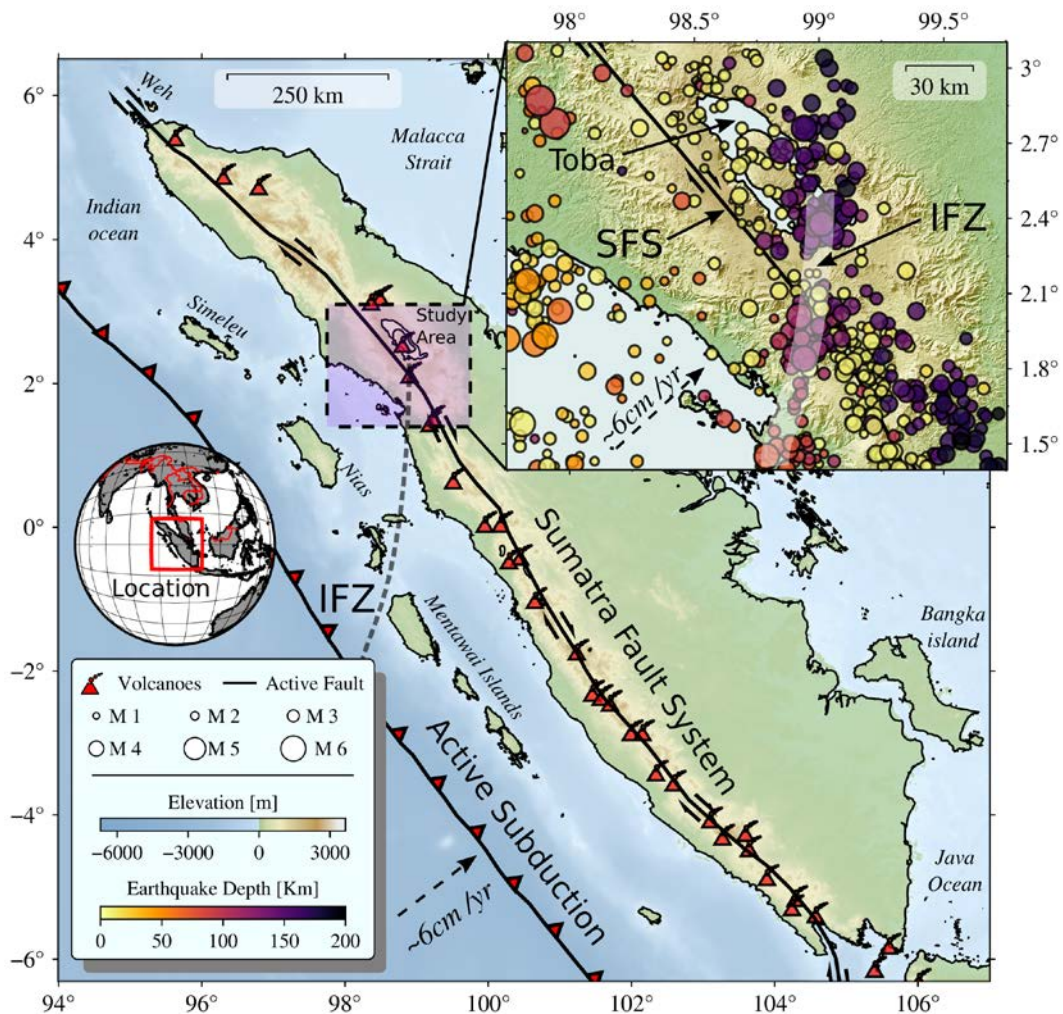


Fig. 1 Map showing the tectonic systems in Sumatra Island that are dominantly controlled by the active subduction with 5 - 6 cm/year directed beneath the Eurasian Plate parallel to the active segmentation from the Sumatra fault [5, 6]. The dashed line follows the line of the Investigator Fracture Zone (IFZ) until beneath Toba Lake from several studies such as Koulakov et al. [3], Liu et al. [4] and Fauzi et al. [9].

Besides the seismicity analysis, our focus was on obtaining a suitable 1-D velocity model that would fit the tectonic Toba system and reveal the relative relocation in order to cluster the specific source from the subduction, the IFZ, and the Toru fault near Toba Caldera. Further, our results are important to update the tectonic system in the

Toba location.

2. RESEARCH SIGNIFICANCE

The results successfully map the down-dip of the active subduction and the IFZ with the possibility of the slab gap location while shallow

activities are from the Toru fault. The presence of the slab was proposed, in that the tear from the IFZ may incorporate with the slab bending and also with a gap in the moderate depth. The results will provide a significant contribution to the existing map of the tectonic system in Toba and its surroundings based on recent seismic activities.

3. MATERIAL AND METHODS

3.1 Data Observation and Location

To explain the tectonic process in Toba and its surroundings, the seismic data was used that

contains the seismic body wave arrival times (P and S phases). The arrival times have been recorded at each permanent seismic station from the Meteorology, Climatology and Geophysics Agency (BMKG, Indonesia) for the last decade. Here, the arrival time is used to determine the appropriate velocity model and relocate the earthquake hypocenter to construct a cluster that maps the recent tectonic condition. A total of 720 earthquake hypocenters from 2009 – 2021 (12 years) are recorded with 72 seismic stations, as shown in Fig. 2.

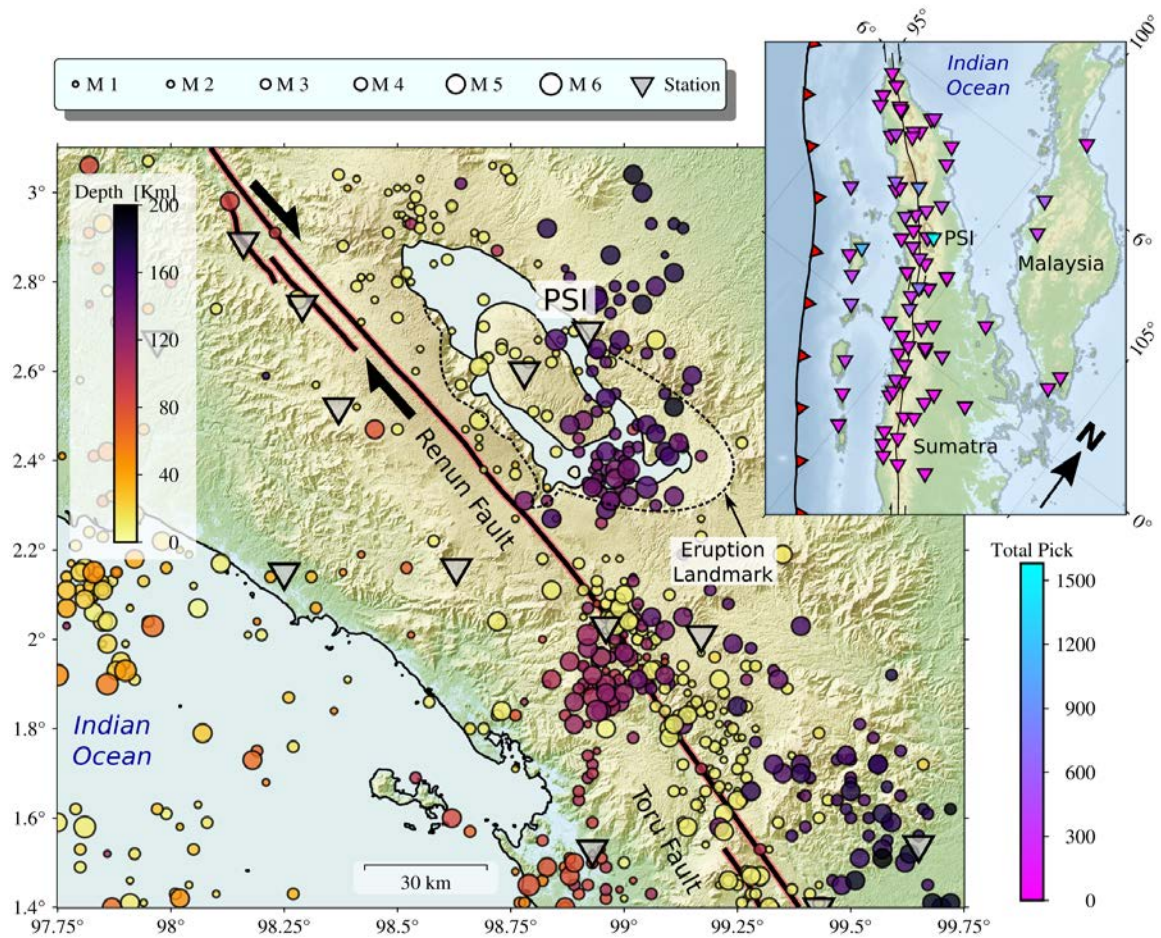


Fig. 2 Seismicity map showing the earthquake distribution in the Toba region and its surroundings at a depth range of 0-200 km. The eruption landmark (dashed line) of Toba is located parallel with Renun fault (red line) that moves with dextral direction. The recording station (gray triangle) when the P and S waves arrive is in the range 0 – 5° (~500 Km) with a total range of P and S picks per station 0 – 1,580 picks (top right panel). The PSI station is categorized as the sensor with highest number of picks with ~1500 total picks.

The earthquake criteria was set such as, (a) the number of seismic phases observed must be 10 with a minimum of 4 S-phases, (b) the hypocenter criteria have depth range at 0 - 200 km, (c) azimuth gap coverage < 200°, and (d) the distance between hypocenters with the seismic station distribution is 0 – 4°. From these criteria, total of

410 earthquakes were obtained from the catalog time 2010 - 2022 that were recorded by 72 stations (Fig. 2). The total seismic phases for hypocenters relocation are 6100 P-phase and 900 S-phase.

3.2 Hypocenter Relocation

Hypocenter location is important to figure the detailed structure that can be used for various seismic studies. However, it requires a good earthquake monitoring network with an appropriate seismic velocity model. Therefore, the error of hypocenter can be reduce significantly with a new location. Here, the optimum model of 1-D seismic velocity were obtained that is suitable for Toba tectonic system. The 1-D velocity model was first estimated by inverting the travel times of the P and S-phase with the hypocenter and station arrival time delay using VELEST [14]. The VELEST algorithm produces the most appropriate solution from all random models to combine the hypocenter velocity in each earthquake sequence and generate a minimum 1-D velocity model.

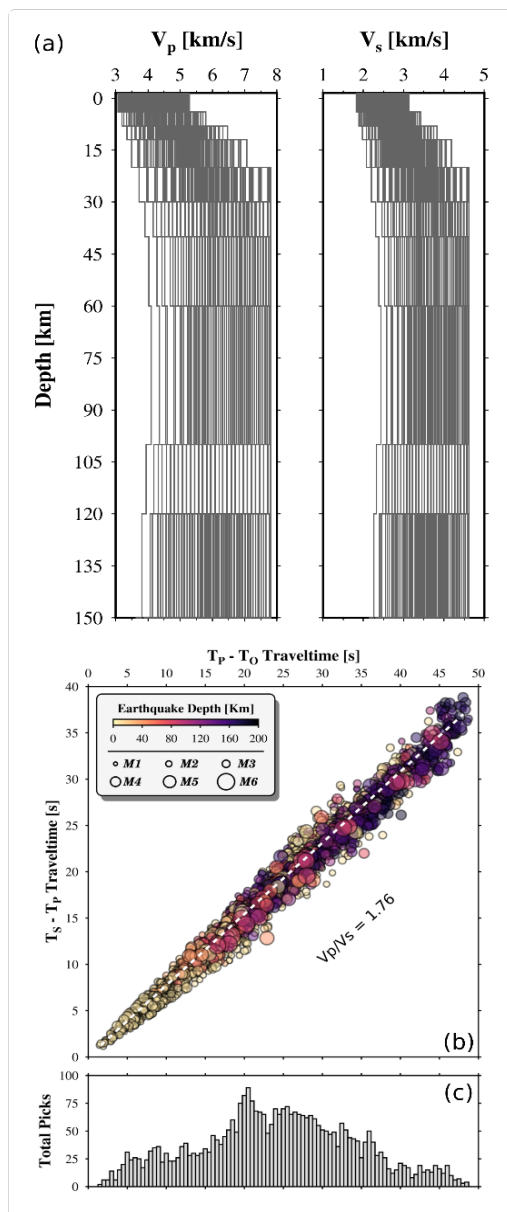


Fig. 3 The initial random model for VELEST processing (a). The wadati diagram shows $T_s - T_p$

and $T_p - T_o$ with the linear trend that has ratio 1.76 as a representative of V_p/V_s (b). Total number of picks is from all seismic stations in the study area with most picks located in the range 15 – 25 s (c).

By using a suitable velocity model from VELEST, the hypocenters were then continued with the HypoDD program [15] to cluster the hypocenter based on the relative relocation. The main algorithm of HypoDD assumes that if there are two earthquakes with a hypocenter distance shorter than the distance to the recording station, then the path between earthquake and station has a similar medium. HypoDD minimizes the residual between the observed and calculated travel time differences in the iterative procedure as shown in Fig. 3. After each iteration, the hypocenter position will be updated and HypoDD minimizes the residual time between the observed and the calculated. The residual time utilizes the time differences in each iteration to group the hypocenters into a cluster.

4. RESULTS AND DISCUSSION

The VELEST processing times using multiple models was started with random initial models. Totally, 100 a priori initial models were gained and simultaneously inverted to obtain appropriate P and S models. The shifting values were set for all initial models by $\pm 5\%$, $\pm 10\%$, and $\pm 15\%$ from the original. The final velocity model is obtained with an average of 5 models produced with the lowest RMS value of 0.0 – 0.9 s.

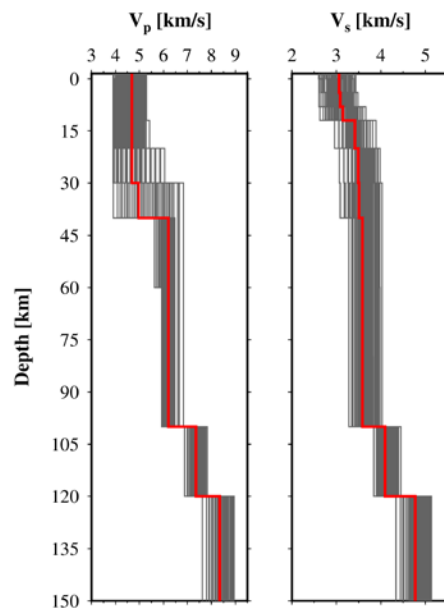


Fig. 4 All inverted velocity models result within the given velocity corridor. The red line is the model with the smallest RMS, and it is considered to be the solution to the velocity model.

P and S velocities increase slowly from shallow depths of < 10 Km with a stable V_p/V_s ratio of around 1.76. The velocity model shown in Fig. 4 is a unique minimum solution because it is given randomly to obtain the most appropriate model according to seismicity conditions in the research area. Furthermore, the updated hypocenter using the double difference method provides more precise hypocenters position and clusters. The parameters used consisted of a maximum hypocentral separation of 30 km, the maximum number of neighbors per event of 50 km, and the minimum number of connections required to determine neighbors was 8 phases. As a consequence to relocate a large number of earthquakes, the least-square conjugate gradient method was chosen as it is more efficient.

The damping parameter was set at a value of 20 to give a CND parameter between 40 and 80 for the majority of the hypocenters obtained, as suggested by Waldhauser [15]. Catalog data are

shown with higher a priori for weighting to obtain the relative hypocenters position of all events during the first six iterations. As many as 88% of the total earthquakes (401 events) were successfully relocated while 103 were not relocated because they did not meet the predetermined criteria. The relocation results show a significant change in earthquake events with an RMS of 0 – 0.5s.

4.1 Hypocenter Relocation

To see the hypocenter change in the position of the hypocenter, three cross sections was set to figure the seismicity in the vertical profile. We set two horizontal lines (A-A' and B-B') and one vertical line (C - C') on the initial data, before and after relocation as show in Fig .5. The cross section shows clusters that follow a subduction slab pattern at a depth of 0 - 200 Km.

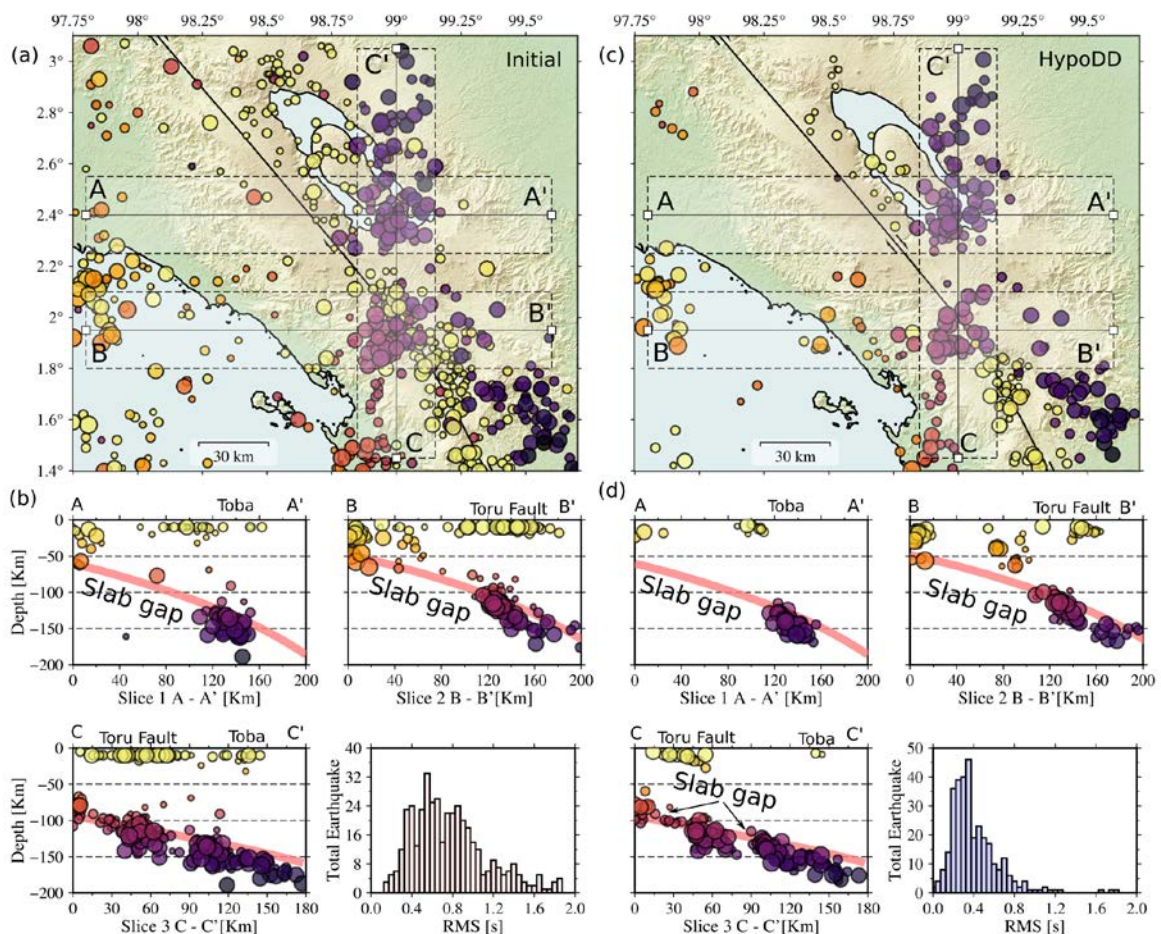


Fig. 5 Map of distribution hypocenter before relocation with three slices (A - A', B - B', C - C') (a). Three cross section profiles from three slices map the initial hypocenters along subduction and the error distribution for earthquake parameters (b). Map of distribution earthquake after relocation with HypoDD with three slices (c). Three cross section profiles from three slice figures and existence of slab gap along subduction after relocation and error distribution that mostly reduce below 0.5s which gain the updated hypocenters quality.

The subduction gap is clearly described in A - A' and B - B' before and after the relocation which indicates that there is a locking zone with a high degree of asperity. However, the improvement of hypocenter quality must be conducted to reduce the hypocenter distribution in order to support the explanation about the recent tectonic system. Our results also shows the significance quality change of hypocenter error which is around 90% of total hypocenter relocation, has $RMS < 1.0s$, while 60% of total hypocenter relocation has $RMS < 0.5s$. Meanwhile, slice C - C' shows the slab gap from the hypocenter distribution in the two zones at a depth of 100 and 120 Km, respectively. The vertical profile of C - C' was set following the IFZ to map the possible slab gap. The relocation of the hypocenters shows the slab from the IFZ incorporated with the slab subduction and has generated more earthquakes than subduction.

4.2 Slab Gap Beneath Toba

To support our results, the earthquake catalog from the International Seismological Center (ISC) was added for the year prior to 2008 [16]. The

ISC catalogue has been well-reviewed and can be used to explain the tectonic system in a specific area [17]. In addition, the focal mechanism from the Global Centroid Moment Tensor (GCMT) [18] was also added to see the mechanism of a slab features beneath Toba, as shown in Fig. 6. The combined data were then cross-sectioned again to map the regional seismicity, such as the existence of the slab folding with a seismic gap by cutting according to the dip of focal distribution on the thrusting mechanism of the subduction system.

Slab folding is categorized as the slab with dip and strike in the drastic variations that are suggested as the continuous feature beneath Toba [3, 9]. Moreover, Pesicek et al. [19] described the slab as folding beneath the northern part of Sumatra, starting at depths of 150 to 500 km. Another possible assumption of the slab gap from the IFZ is tied to the area having low velocities. For example, Fauzi et al. [9] found another subducted IFZ beneath Nias Island and adjacent areas. The IFZ subducted seamounts have elevations of 1,000 – 1,500 m above the seafloor in the Indian Ocean and its surrounding.

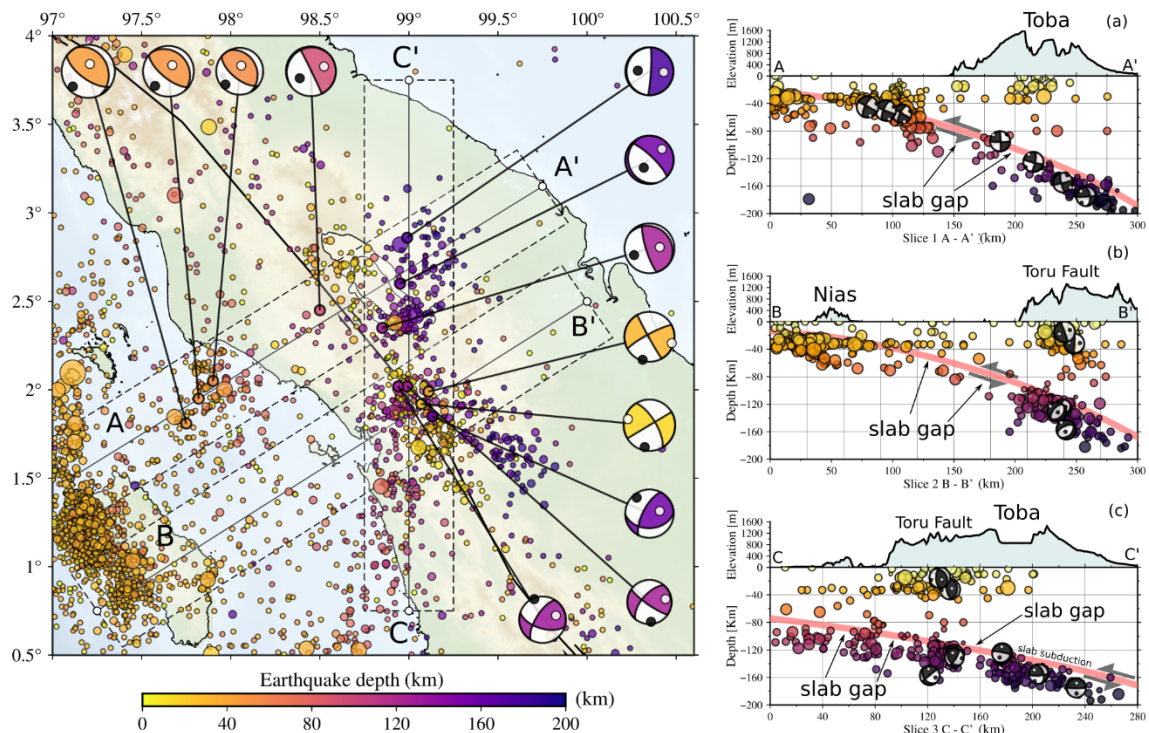


Fig. 6 Map of the regional seismotectonics of Toba and its surrounding area with three vertical slices A – A', B- B', and C – C' with data combined between global seismicity from ISC (1964 – 2008) [23], earthquake focal mechanisms from Global CMT (1980 – 2008) [24] and hypocenter relocation results. Vertical profiles from three slices beneath Toba (a) A – A' slice and (b) B – B' slice figure the SW – NE vertical profiles of Toba seismotectonics while (c) C – C' slice figures the S – N vertical profiles of Toba seismotectonics.

To elucidate the tectonic processes, three slices were given to figure the Toba seismicity in the

vertical profiles. The A - A' oblique cross section shows an absence of seismic activities that also

features a slab gap between the interface and intraslab zone. The B - B' oblique cross-section also features what is clearly a gap after the interface zone until the intraslab zone, while the high degree of activities can be found beneath Nias Island as the fore-arc island formation that forms the accretionary prism structure. On the C - C' vertical cross-section, the IFZ system constructs a slab structure with a possibility gap in the depth range 100 – 150 Km. The IFZ systems also appears as if it is incorporated with the subduction zone, with slab contours much deeper.

The condition is jointly located with the fracture zone in the thick oceanic crust and also may indicate negative velocity perturbations. Furthermore, the age differences across the IFZ provide a density contrast that may possibly be generate by various mechanisms and a slab gap. Liu et al. [4] propose that the slab in the north is warmer and more buoyant, while south part is colder and dense. The oceanic plate in the western part from the IFZ line is relatively younger than the slab east of the IFZ by up to ~15 Ma [12].

4.3 Slab Tear

The IFZ in the direction vertically beneath Toba may have made a possible slab tear beneath Toba. Several studies have assumed the existence of slab tear beneath Toba, although to our knowledge no reasonable evidence has been presented [2, 3, 4]. A possible slab tear can be assumed by following the slab dip curvature, which varies from the north to the south. Fauzi et al. [9] suggested that there is a tear in the slab from the seismicity that has the same depth as that suggested by recent tomographic model from Liu et al. [4]. Hall and Spakman [20] also suggested the slab tear in the northern part of IFZ dips more steeply to the east. Koulakov et al. [3] proposed that the presence of the IFZ has made a slab tear beneath northern Sumatra with significant low-velocity zones in the overlying mantle wedge.

Fauzi [9] figured that the density contrast based on oceanic crustal age differences across the IFZ and the right lateral shear stress on the slab may be responsible for the potential tearing of the subducted slab. A study by Page et al. [21] found the existence of slab tear by analyzing the volcanoes south of Toba are located along the SFS; in contrast, the volcanoes north of Toba are shifted to the east of the SFS. Page et al. [21] showed also that the dip of the northwest slab is shallower than southeast slab, which can explain the unusual volcanic activity in the Toba area [3].

Furthermore, the possible serpentization of the uppermost mantle with fractures and transform faults beneath IFZ can make the slab rheologically weak. The slab tear is different from

the orientations of the IFZ north of the NNE Wharton Fossil Ridge [11, 14]. The IFZ activities can be categorized as the active tectonic system in Sumatra and may generate potential major events in the near future. Based on that, a future mitigation program for IFZ earthquakes distribution can be studied and conducted by using several studies incorporating such as seismic hazard [22, 23], microtremor [24], and social education [25].

5. CONCLUSIONS

Toba lake has formed as a result of tectonic activities over several centuries. The tectonic process has generated massive seismic activities that generate an IFZ system and influence the volcanic activities beneath Toba. The geometry of the IFZ that incorporated with slab subduction indicated a bend portion with high seismicity. The IFZ is subducted at an oblique angle of ~65° below the Toba caldera, and the direction of the fracture zone trend near the trench is almost parallel to the convergence vector. A possible slab tear with slab gap from hypocenter relocation can be found along IFZ as the consequence of rheologically weak structure which varies from the north to the south. The finding result can be used as the mitigation study for the earthquake activities of the IFZ.

7. REFERENCES

- [1] Chesner, C. A., & Rose, W. I., Stratigraphy of The Toba Tuffs and The evolution of The Toba Caldera Complex, Sumatra, Indonesia. *Bulletin of Volcanology*, Vol. 53, Issue 5, 1991, pp. 343-356.
- [2] Masturyono, R. McCaffrey, D. A. Wark, S. W. Roecker, Fauzi, G. Ibrahim, and Sukhyar, Distribution of magma beneath the Toba caldera complex, north Sumatra, Indonesia, constrained by three-dimensional P wave velocities, seismicity, and gravity data, *Geochem. Geophys. Geosyst.*, Vol. 2, Issue 1014, 2001, pp. 1-24.
- [3] Koulakov, I., Yudistira, T., & Luehr, B. G., P, S velocity and VP/VS ratio beneath the Toba caldera complex (Northern Sumatra) from local earthquake tomography, *Geophysical Journal International*, Vol. 177, Issue 3, 2009, pp. 1121-1139.
- [4] Liu, Y., Suardi, I., Huang, X., Liu, S., & Tong, P., Seismic velocity and anisotropy tomography of southern Sumatra. *Physics of the Earth and Planetary Interiors*, Vol. 316, 2021, pp. 1-11.
- [5] Prawirodirdjo, L., McCaffrey, R., Chadwell, C. D., Bock, Y., & Subarya, C., *Geodetic Observations of An Earthquake Cycle at The*

- Sumatra Subduction Zone: Role of Interseismic Strain Segmentation, *Journal of Geophysical Research: Solid Earth*, Vol. 115, B3414, 2010, pp. 1-15.
- [6] Sieh K. & Natawidjaja D., Neotectonics of the Sumatran fault, Indonesia, *Journal of Geophysical Research: Solid Earth*, Vol. 105, Issue 12, 2000, pp. 28295–28326.
- [7] Muksin, U., Bauer, K., & Haberland, C., Seismic Vp and Vp/Vs structure of the geothermal area around Tarutung (North Sumatra, Indonesia) derived from local earthquake tomography. *Journal of volcanology and geothermal research*, Vol. 260, 2013, pp. 27-42.
- [8] Pasari, S., Simanjuntak, A. V., Mehta, A. & Sharma Y., A synoptic view of the natural time distribution and contemporary earthquake hazards in Sumatra, Indonesia. *Natural Hazards*, Vol. 108, Issue 1, 2021, pp. 309-321.
- [9] Fauzi, McCaffrey, R., Wark, D., Sunaryo, & Prih Haryadi, P. Y., Lateral variation in slab orientation beneath Toba Caldera. *Geophysical Research Letters*, Vol. 23, 1996, pp. 443–446.
- [10] Sakaguchi, K., Gilbert, H., & Zandt, G., Converted wave imaging of the Toba Caldera, Indonesia. *Geophysical research letters*, Vol. 33, Issue 20, 2006, pp. 1-6.
- [11] Jaxybulatov, K., Shapiro, N. M., Koulakov, I., Mordret, A., Landès, M., & Sens-Schönfelder, C., A large magmatic sill complex beneath the Toba caldera. *science*, Vol. 346, Issue 6209, 2014, pp. 617-619.
- [12] Lange, D., Tilmann, F., Rietbrock, A., Collings, R., Natawidjaja, D. H., Suwargadi, B. W., & Ryberg, T., The fine structure of the subducted investigator fracture zone in western Sumatra as seen by local seismicity. *Earth and Planetary Science Letters*, Vol. 298 Issue 1-2, 2010, pp. 47-56.
- [13] Syracuse, E. M., & Abers, G. A., Global compilation of variations in slab depth beneath arc volcanoes and implications. *Geochemistry, Geophysics, Geosystems*, Vol. 7, Issue 5, 2006, pp. 1-18.
- [14] Kissling, E., Ellsworth, W. L., Eberhart-Phillips, D., & Kradolfer, U., Initial reference models in local earthquake tomography. *Journal of Geophysical Research: Solid Earth*, Vol. 99, Issue B10, 1994, pp. 19635-19646.
- [15] Waldhauser, F., hypoDD—A Program to Compute Double-Difference Hypocenter Locations (hypoDD version 1.0-03/2001). US Geol. Surv. Open File Rep., Open file report 01-113, 2001, pp. 1-25.
- [16] International Seismological Center (ISC) earthquakes data (1964 – 2008) <http://www.isc.ac.uk/isc-ehb> (accessed Oct. 1, 2022).
- [17] Weston, J., Engdahl, E. R., Harris, J., Di Giacomo, D., & Storchak, D. A., ISC-EHB: reconstruction of a robust earthquake data set. *Geophysical Journal International*, Vol. 214, Issue 1, 2018, pp. 474-484.
- [18] Global Centroid Moment tensor (GCMT) earthquakes data (1980 – 2008) <http://www.globalcmt.org/CMTsearch.html> (accessed Oct. 1, 2022)
- [19] Pesicek, J. D., Thurber, C. H., Widiyantoro, S., Engdahl, E. R., & DeShon, H. R., Complex slab subduction beneath northern Sumatra. *Geophysical Research Letters*, Vol. 35, Issue 20, 2008, pp. 1-5.
- [20] Hall, R., & Spakman, W., Mantle structure and tectonic history of SE Asia. *Tectonophysics*, Vol. 658, 2015, pp 14-45.
- [21] Page, N. G. N., Bennett, J. D., Cameron, N. R., Bridge, D. M. C., Jeffery, D. H., Keats, W., & Thaib, J., A review of the main structural and magmatic features of northern Sumatra. *Journal of the Geological Society of London*, Vol. 136, Issue 5, 1979, pp. 569–577.
- [22] Muksin, U., Riana, E., Rudiyanto, A., Bauer, K., Simanjuntak, A. V. H., & Weber, M., Neural network based classification of rock properties and seismic vulnerability. *Global Journal of Environmental Science and Management*, Vol. 9, Issue 1, 2022, pp. 15-30.
- [23] Pasari, S., Simanjuntak, A. V., Mehta, A., & Sharma, Y., The current state of earthquake potential on Java Island, Indonesia. *Pure & Applied Geophysics*, 178(8), 2021, pp.2789-2806.
- [24] Asnawi, Y., Simanjuntak, A. V., Muksin, U., Okubo, M., Putri, S. I., Rizal, S., & Syukri, M., Soil Classification in A Seismically Active Environment Based on Join Analysis of Seismic Parameters. *Global Journal of Environmental Science and Management*, Vol. 8, Issue 3, 2021, pp. 297-314.
- [25] Asnawi, Y., Simanjuntak, A., Muksin, U., Rizal, S., Syukri, M., Maisura, M., & Rahmati, R. (2022). Analysis of Microtremor H/V Spectral Ratio and Public Perception for Disaster Mitigation. *International Journal of GEOMATE*, 23(97), 2022, pp. 123-130.